

ECHO: Ego-Centric modeling of Human-Object interactions

Ilya A. Petrov^{1,2}Vladimir Guzov^{1,2}Riccardo Marin^{3,4}Emre Aksan⁵Xu Chen⁵Daniel Cremers^{3,4}Thabo Beeler⁵Gerard Pons-Moll^{1,2,6}¹University of Tübingen, Germany²Tübingen AI Center, Germany³Technical University of Munich, Germany⁴Munich Center for Machine Learning, Germany⁵Google, Switzerland⁶Max Planck Institute for Informatics, Saarland Informatics Campus, Germany

Input: 3-point tracking
(Head and Wrists)

Output: \mathcal{H} - \mathcal{O} interaction

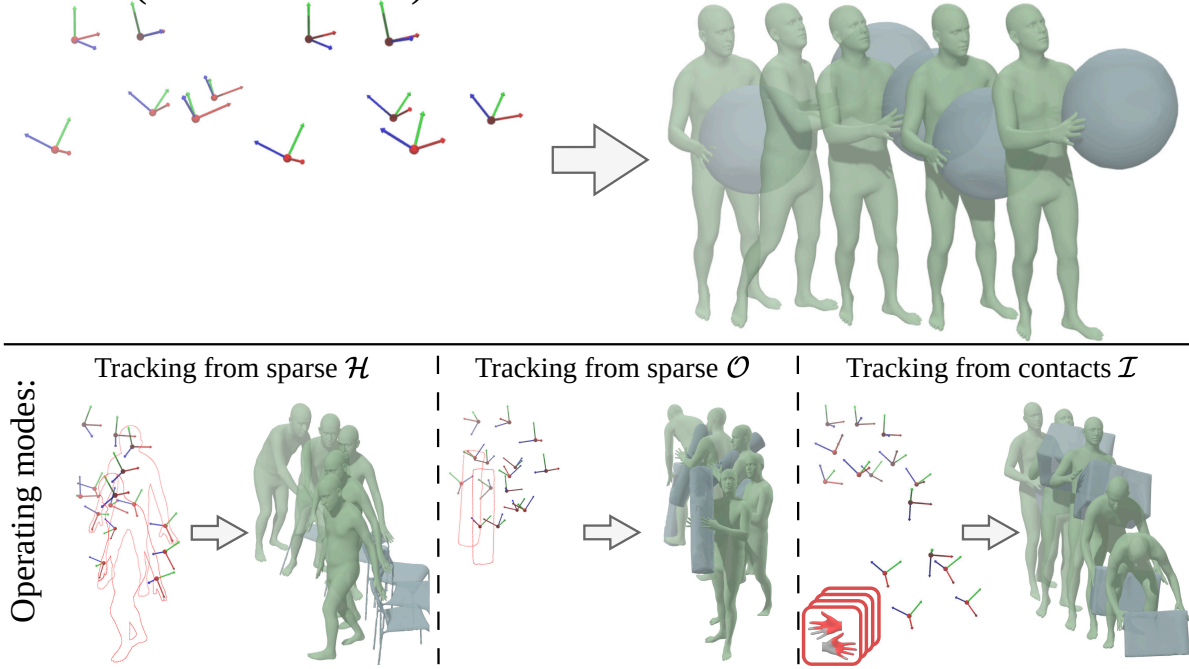


Figure 1. **ECHO**. Wearable devices like smart glasses, watches, and rings are becoming more and more affordable at the customer level. But what can be inferred from such a sparse set of sensors? ECHO is the first model to recover Human-Object Interaction sequences (top) from sparse 3-point tracking. Our method is flexible and can operate in different modes (bottom), for example, incorporating available information (shown in red) of human, object, or contact, even when it is available for just a few frames of the sequence.

Abstract

Modeling human-object interactions (HOI) from an ego-centric perspective is a largely unexplored yet important problem due to the increasing adoption of wearable devices, such as smart glasses and watches. We investigate how much information about interaction can be recovered from only head and wrists tracking. Our answer is ECHO (Ego-Centric modeling of Human-Object interactions), which, for the first time, proposes a unified framework to recover three modalities: human pose, object motion, and contact from such minimal observation. ECHO employs a Diffusion Transformer architecture and a unique three-variate diffu-

sion process, which jointly models human motion, object trajectory, and contact sequence, allowing for flexible input configurations. Our method operates in a head-centric canonical space, enhancing robustness to global orientation. We propose a conveyor-based inference, which progressively increases the diffusion timestamp with the frame position, allowing us to process sequences of any length. Through extensive evaluation, we demonstrate that ECHO outperforms existing methods that do not offer the same flexibility, setting a state-of-the-art in egocentric HOI reconstruction.

1. Introduction

Wearable sensors have become increasingly present in our lives, from wristbands to smart glasses [65], from AR helmets [32] to rings. These devices not only enable XR/VR, but also act as daily companions, tracking our movements and serving as smart assistants. Developing algorithms that can perceive and understand user activities and interactions from such sparse signals is a prominent research direction, with implications in healthcare, entertainment, robotics, and ultimately, Spatial AI. Thanks to the advancements in wearable SLAM [66], for example, it is possible, to reconstruct the surrounding environment on the way. This enables algorithms to shift from an egocentric to a holocentric perspective, albeit with the assumption of static scenes. Similarly, it has been shown that it is possible to reconstruct the users' motion from sparse sensors [27, 100]. Despite these advancements, only a limited number of recent works [25, 93] have considered egocentric human-object interaction. Existing methods have significant limitations, as they rely on a substantial amount of additional information, such as RGB images or pre-scanned scenes, or require the use of specialized capturing suits. Moreover, these approaches model the interaction as a regression problem, which disregards the underconstrained nature of the task.

Our work is inspired by the observation that, to date, no system has been developed to track human-object interaction in a sparse egocentric setup – namely, recovering a human *and* an interacted object motions, relying solely on wrists and head tracking. The result of our efforts is ECHO, the first method to solve for human and object motion sequences jointly, relying only on 3-point tracking. ECHO predicts the human, object, and interaction (i.e., contact). It can also leverage *sparse* observations of any of these modalities to constrain the prediction of the others (e.g., inferring human and object motion from partial contact information), using 3-point tracking as a constant anchor. To do so, we propose several paradigm shifts. First, ECHO does not rely on a world coordinate system as some prior works [10, 27], but reasons in a head-centric space. This makes the model more robust to a global orientation of the interaction sequence. Secondly, our tri-variate diffusion formulation enables to train on a combination of HOI datasets with human motion ones, showing high quality in modeling the human motion. Finally, we propose and implement a conveyor-based approach for training and inference. Unlike the standard per-window approach, it assigns a unique timestamp to every frame for every modality. This allows for inference on arbitrarily long sequences and the usage of sparse information (e.g., due to noisy observations).

ECHO relies on weak assumptions, making it flexible and adaptable to diverse settings. Its triple-way diffusion formulation enables the incorporation of further information (e.g., human tracking from IMUs, object tracking

from RGB, ...), making ECHO a universal method, potentially deployable to other autonomous agents as well (e.g., robots). ECHO achieves state-of-the-art, outperforming competitors that lack the same flexibility. Our detailed ablation demonstrates the effectiveness of our design choices, which we believe will be instrumental for further research and will have a concrete impact on the egocentric research.

Our key contributions can be summarized as follows:

- We present the first method to model human-object interactions from wearable 3-point trackers. By design, the model is able to solve a set of different tasks of human and object motion inference common for AR and VR.
- We propose a novel universal generative model that jointly predicts human and object motion. The model is trained to support partial observations and perform inference for arbitrary long sequences using conveyor.
- We define a new head-centric human-object representation that results in more precise interaction prediction.
- The code and trained models will be released, providing the community with a strong foundation in the egocentric human-object interaction reconstruction research.

2. Related Work

Egocentric Motion Reconstruction. The use of body-worn and head-mounted sensors for human motion reconstruction is an emerging area of research. Earlier methods used the camera on the body to recover hand position [5, 8, 21, 55, 70, 97], or the camera heading towards the person to recover the full-body motion [1, 40, 45, 51, 52, 69, 77, 91]. These approaches focus only on joints angles, and do not track the position in the scene.

Another line of work utilizes body-worn sensors, such as EMs [41], EMGs [12], and inertial measurement units (IMUs) [79]. Among these works, IMUs received the most popularity [4, 34, 39, 58, 80, 90, 95, 96, 106], integrating physical constraints, and reducing the number of required sensors. However, they compute the body's position through double integration of acceleration data, which leads to error accumulation.

An advancement came with HPS [24], the first method to fuse IMU-based pose tracking with camera localization to estimate both local and global body pose in the scene. Follow-up works enhanced this framework by enabling scene scanning [15, 50], scaling datasets [31, 54], and reducing the number of required sensors [13, 36, 44, 82, 104].

Generative diffusion models enabled the synthesis of realistic body motion from the underconstrained input [10, 18, 81]. Methods like EgoEgo [46] demonstrated generation of full-body motion from a head trajectory. Further works [19, 27, 94] made use of additional modalities, such as video, scene point cloud, and hands detections.

We adopt a similar approach and include sparse head and hand conditioning in our model. However, in contrast to the

aforementioned methods, our approach models dynamic interactions with objects in the scene. This enables complete reconstructions of human activity in real-world settings.

HOI Reconstruction and Synthesis. Earlier works in HOI reconstruction and synthesis have primarily focused on human-centric modeling, generating only human motion while assuming static environments [28, 29, 33, 57, 75, 87, 102]. These methods do not model the changes of the scene, such as object position, which limits their applicability in real-world scenarios.

More relevant to our work are methods that model dynamic human-object interactions. A significant subset of these approaches uses text or action label as a conditioning input [9, 17, 48, 49, 62, 73, 89]. While this offers flexibility and creative freedom, it often lacks the precision needed for fine-grained motion control and detailed interactions. Other methods, such as TRUMANS [37] condition on the surrounding scene, improving realism and control at the cost of requiring prior knowledge of the scene. More realistic and precise results are provided by methods conditioned on visual input, such as RGB [14, 20, 59, 78, 83–86, 99], including multiple cameras [38, 98], RGBD [6, 35] or a combination of text and image [92]. However, using an external camera requires constantly observing the scene from a third-person view, which limits scalability.

Another line of research focuses on generating interactions based on partial information, such as past observations [23, 88], object positions [7, 43, 47], or human pose [63, 101]. A notable follow-up is TriDi [64], which models the joint distribution of a human, object and interaction, allowing conditioning on either. However, it does not incorporate temporal modeling and is limited to per-frame estimation. We extend TriDi’s trilateral diffusion to capture temporal dynamics. This enables ECHO to model both human-only motion and joint human-object interactions, as well as allows for flexible configuration of input modalities.

Egocentric HOI Reconstruction methods Most methods that model human-scene interaction from egocentric data assume static environments [15, 24, 44, 50], and are therefore less relevant to our focus on dynamic interaction.

The closest approach to ours is iReplica [25], the only existing method that considers both humans and dynamic objects in an egocentric scenario. However, iReplica has significant limitations: it primarily targets interactions with large objects and requires extensive setup, including full-body IMUs and a complex initialization process. Our method is the first to produce fully unconstrained human-object interaction capable of handling objects of disparate types and sizes without motion limitations, all from easy-to-use 3-point wearable trackers, making it practical for everyday scenarios.

3. Method

In this section, we present ECHO – the first approach for joint human-object interaction modeling from sparse egocentric input. Unlike prior works [10, 27, 94] that focus on recovering human motion in egocentric setting, we tackle a more general task of modeling interactions. We propose ECHO, a transformer-based diffusion model that predicts human motion \mathcal{H} , object motion \mathcal{O} , and contact sequence \mathcal{I} from the three-point conditioning. Further sections introduce the representations for all the modalities (Sec. 3.1), and describe our formulation of the diffusion process, architecture, and training (Sec. 3.2). Finally, we present the inference conveyor that we adopt for an online inference with an arbitrary sequence length (Sec. 3.3).

3.1. Modalities Representation

Head-centric modeling.

The key design choice for our method was selecting the coordinate system for the network’s output. Although a global coordinate frame might seem like a natural choice for modeling human-object interactions, we found that it introduces significant bias from the overall sequence orientation and does not accurately reflect our egocentric setting.

Instead, we propose to express the global transformation of both human and object with respect to human’s head position and orientation in the first frame of an inference window $((\mathbf{T}_{head})^{-1})$, with its height axis oriented parallel to the gravity axis. We illustrate the transformation in Figure 2. Our head-centric representation makes the model robust to global orientation of the sequence and enhances its ability to generalize across longer motion sequences. As our ablation study demonstrates, this approach simplifies training and improves the quality of the results.

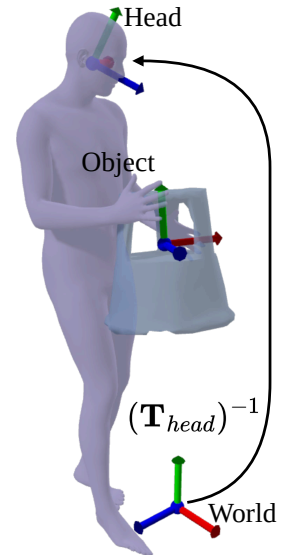


Figure 2. **Head-centric representation.** ECHO operates in a head-centric coordinate system. This choice removes spatial bias from the global configuration.

Object. For every object we assume that its canonical mesh is given to the model as an input. Hence we represent the object as a sequence of its global $SE(3)$ transformations, consisting of rotation and translation pairs in the aforementioned reference system $\mathbf{T}_{\mathcal{O}} = (R_{\mathcal{O}}, t_{\mathcal{O}})$. Follow-

ing [105], we convert all rotations to \mathbb{R}^6 .

Thus a sequence of N object poses is denoted as:

$$\mathcal{O} = \{\mathbf{T}_{\mathcal{O}}^{1..N}\} \quad (1)$$

To represent the object’s class and geometry, we encode the class label in a one-hot encoded vector $\mathbf{y}_{\mathcal{O}}$, and extract a feature vector $\mathbf{f}_{\mathcal{O}} \in \mathbb{R}^{1024}$ from the canonicalized object vertices $\mathbf{V}_{\mathcal{O}}$ using PointNext [67]. The resulting pair $\mathcal{C}_{\mathcal{O}} = (\mathbf{y}_{\mathcal{O}}, \mathbf{f}_{\mathcal{O}})$ is used as a global conditioning for ECHO.

Human. To represent the human body, SMPL-X [60] is the natural choice. SMPL-X is a parametric body model that can be seen as a function $SMPL(\mathbf{T}_{\mathcal{H}}, \boldsymbol{\theta}, \beta, \psi)$ of root pose and orientation $\mathbf{T}_{\mathcal{H}} \in SE(3)$, pose $\boldsymbol{\theta}$, shape β , and facial parameters ψ . The function $SMPL$ maps parameters to posed vertices $\mathbf{V}_{\mathcal{H}} \in \mathbb{R}^{10475 \times 3}$ of the predefined template mesh. The pose vector $\boldsymbol{\theta}$ is a concatenation of parameters for body, hands, eyes, and jaw poses in axis-angle format. As our method focuses on the realistic full-body interactions, we model only the body pose $\boldsymbol{\theta}_{\mathcal{H}} \in \mathbb{R}^{21 \times 6}$ of the pose vector and assume known shape parameters β , and for the rest of the manuscript, we simplify the notation to $SMPL(\mathbf{T}_{\mathcal{H}}, \boldsymbol{\theta}_{\mathcal{H}})$. Hence, we define a sequence of human motion with N frames as:

$$\mathcal{H} = \{[\mathbf{T}_{\mathcal{H}}, \boldsymbol{\theta}_{\mathcal{H}}]^{1..N}\} \quad (2)$$

Contacts. While contact prediction may seem redundant at first — since it can be derived from the spatial relationship between the human and the object — our ablation study demonstrates its value. We found it provides a useful, explicit training signal and enables self-supervised inference guidance. Furthermore, it can be used to control the sampling process, such as by providing sparse contact observations as an additional conditioning.

We represent the contact as a vector $\mathbf{c}_{\mathcal{I}} = \{d(p, \mathbf{V}_{\mathcal{O}}) \leq \tau_c | p \in \mathbf{P}_c, \mathbf{P}_c \subset \mathbf{V}_{\mathcal{H}}\}$ with binary contact map for a fixed set of points \mathbf{P}_c uniformly sampled from SMPL-X vertices, where $d(p, \mathbf{V}_{\mathcal{O}}) = \min_{v \in \mathbf{V}_{\mathcal{O}}} \|p - v\|_2$. Additionally, we provide contact labels for the foot-floor contact of both feet. A set of contact maps for a sequence is defined as:

$$\mathcal{I} = \{\mathbf{c}_{\mathcal{I}}^{1..N}\} \quad (3)$$

Ego-centric conditioning. ECHO uses standard ego-centric three-point conditioning [10]. The method is conditioned on orientation $\mathbf{R}_{3p} \in \mathbb{R}^{3 \times 6}$ and coordinates $\mathbf{J}_{3p} \in \mathbb{R}^{3 \times 3}$ of the head and hands joints. More specifically, we construct the following vector $[\mathbf{R}_{3p}, \boldsymbol{\omega}_{3p}, \mathbf{J}_{3p}, \mathbf{v}_{3p}] \in \mathbb{R}^{54}$, where $\boldsymbol{\omega}_{3p} \in \mathbb{R}^{18}$ is the rotational velocity of three-point conditioning, and $\mathbf{v}_{3p} \in \mathbb{R}^9$ is the coordinate velocity of the head and the two hand joints. An ego-centric conditioning for a sequence is defined as:

$$\mathcal{E} = \{[\mathbf{R}_{3p}, \boldsymbol{\omega}_{3p}, \mathbf{J}_{3p}, \mathbf{v}_{3p}]^{1..N}\} \quad (4)$$

3.2. ECHO model

ECHO models the joint distribution of human motion \mathcal{H} , object motion \mathcal{O} , and contact sequence \mathcal{I} , conditioned on the three-point tracking \mathcal{E} and object features $\mathcal{C}_{\mathcal{O}}$. Below we formulate a three-variate diffusion process that is used to model three modalities within one network and provide details on the underlying network’s architecture.

Background A diffusion process in the context of generative neural networks is divided into two phases. The forward phase progressively adds noise to an original data sample, while the backward phase uses a learned model to recover the sample from the noise. We adopt the formulation of Denoising Diffusion Probabilistic Model (DDPM) [30] in our work with a modification following [68], predicting the original sample by the neural network, instead of predicting the added noise. To achieve this, we parametrize the reverse process by a denoising neural network \mathcal{D}_{ψ} that is trained to recover the original sample \mathbf{z}_0 from the noised sample \mathbf{z}_t at timestep t given the condition c . Defining for brevity $\mathbb{E}_p \equiv \mathbb{E}_{\mathbf{z}_0 \sim p_{data}}$, $\mathbb{E}_t \equiv \mathbb{E}_{t \sim \mathcal{U}\{0, \dots, T\}}$, and $\mathbb{E}_q \equiv \mathbb{E}_{\mathbf{z}_t \sim q(\mathbf{z}_t | \mathbf{z}_0)}$ we obtain the training objective (the full definition of forward and backward processes is included in the Sup. Mat.):

$$\min_{\psi} \mathbb{E}_p \mathbb{E}_t \mathbb{E}_q \|\mathcal{D}_{\psi}(\mathbf{z}_t; c, t) - \mathbf{z}_0\|_2. \quad (5)$$

The original formulation of the diffusion model [30, 72] focuses on generating single modality data, e.g. images. We take inspiration from TriDi [64] and UniDiffuser [3], and formulate a tri-variate diffusion process to better model the mutual dependencies between human and object motion.

Diffusion formulation. We formulate a three-variate diffusion process for human motion \mathcal{H} , object trajectory \mathcal{O} , and sequence of contacts \mathcal{I} , denoting corresponding sets of timestamps as $\mathcal{T}_{\mathcal{H}}, \mathcal{T}_{\mathcal{O}}, \mathcal{T}_{\mathcal{I}}$. We define:

$$\begin{aligned} \mathbb{E}_p &\equiv \mathbb{E}_{(\mathcal{H}^0, \mathcal{O}^0, \mathcal{I}^0) \sim p(\mathcal{H}, \mathcal{O}, \mathcal{I} | \mathcal{E})}, \\ \mathbb{E}_t &\equiv \mathbb{E}_{(\mathcal{T}_{\mathcal{H}}, \mathcal{T}_{\mathcal{O}}, \mathcal{T}_{\mathcal{I}}) \sim \mathcal{U}\{0, \dots, T\}^{N \times 3}}, \\ \mathbb{E}_q &\equiv \mathbb{E}_{\mathcal{H}^{\mathcal{T}_{\mathcal{H}}} \sim q(\mathcal{H} | \mathcal{H}^0), \mathcal{O}^{\mathcal{T}_{\mathcal{O}}} \sim q(\mathcal{O} | \mathcal{O}^0), \mathcal{I}^{\mathcal{T}_{\mathcal{I}}} \sim q(\mathcal{I} | \mathcal{I}^0)} \end{aligned} \quad (6)$$

The key feature of this formulation is that ECHO diffuses the three modalities following three independent time schedules, allowing to vary the input modalities (e.g. one can provide a tracking information for human in addition to three point conditioning and predict object motion and contact sequence corresponding to it). The main minimization objective for parameters ψ of a model ECHO_{ψ} is:

$$\begin{aligned} \mathbb{E}_p \mathbb{E}_t \mathbb{E}_q \|\text{ECHO}_{\psi}(\mathcal{H}^{\mathcal{T}_{\mathcal{H}}}, \mathcal{O}^{\mathcal{T}_{\mathcal{O}}}, \mathcal{I}^{\mathcal{T}_{\mathcal{I}}}; \mathcal{T}_{\mathcal{H}}, \mathcal{T}_{\mathcal{O}}, \mathcal{T}_{\mathcal{I}}; \mathcal{C}_{\mathcal{O}}, \mathcal{E}) \\ - (\mathcal{H}^0, \mathcal{O}^0, \mathcal{I}^0)\|_2 \end{aligned} \quad (7)$$

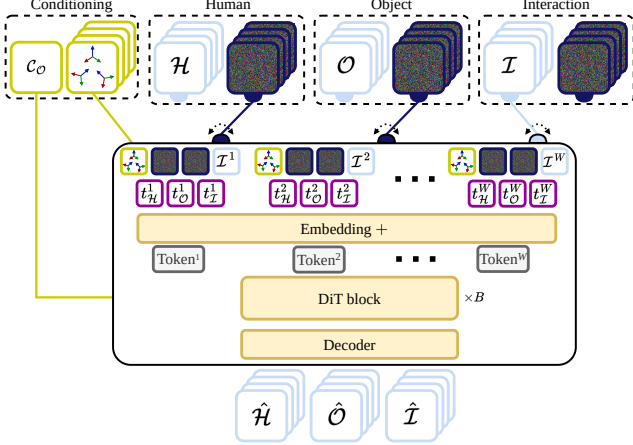


Figure 3. **ECHO overview.** ECHO requires just an object class and head and hands tracking, to predict Human, Object, and Interaction. The input tokens are composed of **condition**, and of either **observed modality**, or **noise** for \mathcal{H} , \mathcal{O} , and \mathcal{I} . For every frame and every modality, we use a unique denoising **time-stamp**, which allows us to adopt Conveyor inference (Sec.3.3). Our model allows flexible input configuration. In the example above we use contacts \mathcal{I} as an **additional input** to the network, that infers the **other modalities** \mathcal{H} , \mathcal{O} , matching the extended condition.

Architecture. We built ECHO denoising network on the diffusion Transformer DiT [61]. The input to the model consists of \mathcal{H} , \mathcal{O} , and \mathcal{I} sequences with a varied amount of noise, ego-centric conditioning \mathcal{E} , object conditioning \mathcal{C}_O , and a set of time stamps for each modality $\{\mathcal{T}_H, \mathcal{T}_O, \mathcal{T}_I\}$. The network predicts the clean sequences for the three input modalities. The crucial aspect of our denoising network is the formulation of the noise schedule. We take inspiration from Diffusion forcing [11] and provide W timestamps for every iteration of the diffusion process (resulting in a total $3 \times W$ timestamps). Hence, we assign individual noise schedules for every frame of the sequence, in contrast to the majority of works in the field, which use a single noise schedule for the entire sequence. This change is actually the key to enabling model flexibility in terms of input variations: by decreasing the current denoising step for known \mathcal{H} , \mathcal{O} or \mathcal{I} , the model can attend to these inputs and predict the rest of the interaction to satisfy it. Moreover, if no known interaction data is present, the model can generate realistic motion that closely matches the provided ego-centric conditioning.

Output. As a benefit of our trilateral diffusion formulation ECHO can be additionally provided with partial interaction observations that cover one of the modalities, e.g. for human motion that would be a sequence of $\mathcal{H}_P = \{[\mathcal{T}_H, \theta_H]_{\{t_1 \dots t_P\}} \mid \{t_1 \dots t_P\} \subseteq \{1 \dots N\}\}$, consisting of pairs of global pose and body pose which may or may not be known on each frame. This feature is useful to additionally constrain the prediction, if we have access to either human tracking (e.g., from IMUs) or object tracking (e.g.,

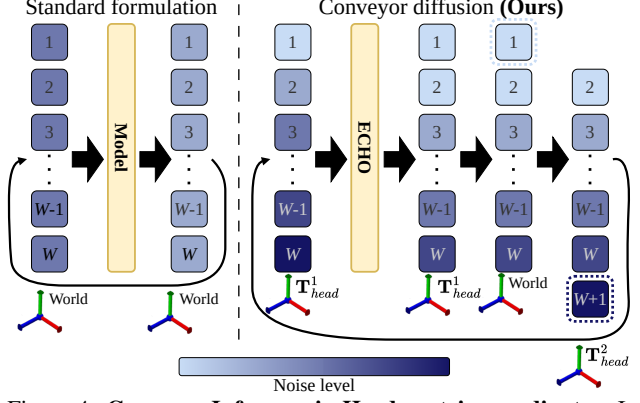


Figure 4. **Conveyor Inference in Head-centric coordinates.** In the standard formulation, all the frames are denoised in parallel with the same timestamp (left). We propose a conveyor diffusion (right), where the denoising timestamp gradually increases towards the end of the window. When the first frame is fully diffused, a new fully noised frame gets appended at the tail, with the appropriate coordinate transform.

from ego-centric camera). As a result, the method outputs the full human-object interaction sequence $\{\hat{\mathcal{H}}, \hat{\mathcal{O}}, \hat{\mathcal{I}}\} = \{[\mathcal{T}_H, \theta_H, \mathcal{T}_O, \mathcal{C}_I]_{1 \dots N}\}$.

Training During training, each frame and input modality – \mathcal{H} , \mathcal{O} , and \mathcal{I} – is noised separately. To support our conveyor-based inference, we implement a special noising schedule where the noise grows toward the end of the current processing window (more details in Section 3.3). The objective function used to train our network is a weighted combination of six loss terms. These include three losses for each diffused modality, a vertex-to-vertex loss for the predicted object, a loss on human joints, and a loss that penalizes foot skating. We provide detailed formulation of losses in the supplementary material. Since the scale of the HOI datasets (14 hours for OMOMO and BEHAVE) is comparatively small, it may not be sufficient to build a robust prior on human motion. Thanks to our model’s flexible versatility in operating modes, we can enrich the HOI-specific training data with motion-only data from the large-scale AMASS [56] dataset. Our ablation study demonstrates the benefit of training on the union of these datasets.

3.3. Inference

To perform diffusion on temporal sequences, recent methods [27, 94] use a sliding window approach, where previous data serves as an anchor for the next predictions. Unlike prior approaches that require the entire sequence to be present from the beginning [10, 76], sliding window enables real-time output, although it requires a post-processing step to stitch the results between windows. Our idea is to take this autoregressive approach further. By adopting a conveyor-based inference strategy [22], we can enable seamless inference for long sequences.



Figure 5. **Qualitative results of ECHO.** Our method (middle) can infer movements well-aligned with the ground truth (left) with a vast variety of objects and motions. Competitors (right) struggle especially with large movements, causing implausible predictions such as penetrations (backpack, suitcase) or flying objects (box, table). Please refer to the supplementary video for dynamic results.

The idea is to denoise the frames in temporal windows with a denoising step that gradually increases from the start to the end of the window (illustrated in Figure 4). Hence, at every denoising step, the earlier frames get denoised faster than the later ones. After the frame at the beginning of the sequence is fully denoised, it is removed, and a new fully noised sample is appended at the end. Since our architecture has independent noise values for every frame within the processing window, we can adapt the conveyor inference with small adjustments in the training procedure.

The conveyor inference introduces two major advancements to ECHO: its ability to run autoregressively on infinitely long sequences, and its capacity to create ‘context frames’ by retaining already denoised frames at the beginning of the queue. By increasing or decreasing the number of context frames, we can control the size of the context to attend to and adjust inference latency, which is important for real-time applications.

Inference guidance To further enhance the quality of generated interactions, we adopt a classifier-based guidance [16] approach at inference time. Following the guidance function’s value, the network’s prediction is modified at every step of the denoising process. We formulate the guidance loss to force the predicted human and object meshes adhere to the predicted binary contact vector $c_{\mathcal{I}}$.

The function therefore includes two terms: one for human-object contacts and one for feet-floor contact.

4. Experiments

Implementation details. The ECHO model has a total of 47.3M parameters that are optimized using AdamW [53] for 400k steps (40 hours) with batch size 256, LR of $1e^{-4}$ on Nvidia H100 GPU. We perform inference with 100 steps of DDPM scheduler achieving a balance between quality and inference time. The average inference speed of ECHO without the guidance is *13.73 ms.* per frame on RTX4090 GPU, which is fast enough for a real-time applications. We use aitviewer [42] and blendify [26] for the visualization.

Datasets. We use a union of BEHAVE [6], OMOMO [47], and AMASS [56] datasets to train and evaluate our method. For BEHAVE and OMOMO we follow official train-test splits. For AMASS we follow the train-test split of EgoAllo [94]. In order to use SMPL-X body model in ECHO we convert BEHAVE sequences from SMPL+H [71] format using the code from [74].

We downsample all the sequences to *30fps* for consistency, as sequences in BEHAVE are only available at this frame rate. During training, we sample windows of size $W = 60$ from the original sequences. For evaluation, we perform continuous inference on the whole sequences.

BEHAVE							
Method	Human			Object			
	MPJPE↓ (mm.)	MPJVE↓	FC	E_{v2v} ↓ (cm.)	E_c ↓ (cm.)	Rot.Diff.↓	Q.Diff.↓
Data	-	-	0.73	-	-	-	-
BoDiffusion [10]	61.4 \pm 1.3	73.3 \pm 1.5	0.94	-	-	-	-
BoDiffusion [10] + Obj	84.1 \pm 1.8	95.9 \pm 2.1	0.96	36.1 \pm 0.7	24.5 \pm 0.6	92.5 \pm 2.5	1.5 \pm 0.1
ECHO (Ours)	<u>61.4</u> \pm 1.0	66.8 \pm 1.1	0.91	29.5 \pm 0.9	17.1 \pm 0.7	82.1 \pm 3.1	1.4 \pm 0.1

OMOMO							
Method	Human			Object			
	MPJPE↓ (mm.)	MPJVE↓	FC	E_{v2v} ↓ (cm.)	E_c ↓ (cm.)	Rot.Diff.↓	Q.Diff.↓
Data	-	-	0.96	-	-	-	-
BoDiffusion [10]	61.2 \pm 1.9	68.5 \pm 2.1	0.98	-	-	-	-
BoDiffusion [10] + Obj	77.3 \pm 2.6	96.4 \pm 3.6	0.99	29.7 \pm 1.6	19.1 \pm 1.0	88.5 \pm 9.4	1.3 \pm 0.1
ECHO (Ours)	<u>64.1</u> \pm 2.9	<u>69.7</u> \pm 3.2	0.95	26.7 \pm 1.9	15.6 \pm 1.1	86.8 \pm 10.3	1.2 \pm 0.2

Table 1. **Comparison with baselines on BEHAVE and OMOMO.** ECHO demonstrates better performance for human-object interaction modeling and competitive motion modeling quality, compared to motion-only BoDiffusion baseline.

Metrics. To evaluate human motion reconstruction quality, we use standard mean per-joint position error (MPJPE) and velocity error (MPJVE [104]), and foot contact measure (FC) [46, 94]. For assessing the quality of object reconstruction, we compute vertex-to-vertex error E_{v2v} [63, 88], center error E_c [63], rotation difference (Rot. Diff.), and quaternion difference (Q. Diff.) [88]. We provide a detailed definition of metrics in the Sup. Mat.

4.1. Comparison with baselines

Baselines. ECHO is the first approach for end-to-end modeling of human-object interactions in the ego-centric setting. Thus, to comprehensively evaluate its performance, we pick several existing methods specializing in ego-centric motion modeling as baselines, and design a modification for HOI modeling on top, posing a significant challenge for our method. We compare with **EgoAllo** [94], one of the recent methods for motion prediction in an ego-centric setting. Although it only relies on the head tracking, it is also designed to use hand guidance for improving the hand tracking. We also compare against **BoDiffusion** [10], which is built on top of DiT [61], processing a concatenation of input tracking and noisy motion per-timestamp, while this latter is embedded into the network as global conditioning. To evaluate the quality of HOI prediction, we build a baseline on top of BoDiffusion, integrating object modeling, and refer to this method as **BoDiffusion+Obj**. We modify the BoDiffusion network to process the object poses and conditioning. We do so by concatenating the global object transformation to the tokens with human motion and ego-centric conditioning, and concatenating object shape embedding and class information to the global conditioning. For fair comparison, we train ECHO and the baselines on the union of AMASS, BEHAVE, and OMOMO.

Method	AMASS		
	MPJPE↓	MPJVE↓	FC \uparrow ^{1.0}
EgoAllo [94]	116.5 \pm 2.1	-	1.0
BoDiffusion [10]	67.0 \pm 1.3	78.7 \pm 1.5	1.0
BoDiffusion [10] + Obj	91.5 \pm 4.2	115.5 \pm 5.9	1.0
ECHO (Ours)	93.9 \pm 8.7	109.7 \pm 4.2	1.0

Table 2. **Quality of motion generation.** ECHO demonstrates competitive performance compared to specialized motion-only baselines, outperforming EgoAllo. Notably, our method performs on par or better than BoDiffusion+Obj, proving its capability to generalize beyond HOI-specific data.

HOI generation. We compare the quality of human-object interaction (HOI) reconstruction on the test sets of BEHAVE and OMOMO. The results are reported in Table 1, which shows the mean and variance across four runs. ECHO significantly outperforms BoDiffusion+Obj in both human and object prediction quality. Notably, the human motion quality of ECHO is on par with, or even surpasses, BoDiffusion, a model trained specifically for human motion reconstruction. We also include qualitative comparisons with baselines in the supplementary video.

Motion generation. While ECHO is designed for human-object interaction, it is also crucial that the method can robustly reconstruct human motion. To focus our evaluation on motion quality, we compare ECHO against models specifically designed for motion synthesis on the AMASS dataset. The results are reported in Table 2, including mean and variance across four runs. As shown, our method performs slightly worse than the original BoDiffusion but outperforms EgoAllo and BoDiffusion+Obj, which demon-

Mode	%	BEHAVE			
		Human		Object	
		MPJPE↓	MPJVE↓	E_{v2v} ↓	E_c ↓
ECHO		61.4 \pm 1.0	66.8 \pm 1.1	29.5 \pm 0.9	17.1 \pm 0.7
Sparse \mathcal{H} available	1	59.9 \pm 0.8	65.4 \pm 0.7	29.4 \pm 0.9	17.2 \pm 0.7
	5	57.6 \pm 0.7	63.0 \pm 0.8	29.3 \pm 0.8	17.1 \pm 0.5
	10	54.2 \pm 0.6	59.4 \pm 0.7	29.2 \pm 0.6	17.0 \pm 0.4
	25	46.3 \pm 0.4	51.1 \pm 0.4	29.0 \pm 0.5	16.9 \pm 0.5
	100	-	-	28.0 \pm 0.1	16.1 \pm 0.1
Sparse \mathcal{O} available	1	61.2 \pm 0.7	66.6 \pm 0.8	28.6 \pm 0.7	17.0 \pm 0.4
	5	61.1 \pm 0.7	66.6 \pm 0.8	27.0 \pm 0.6	16.4 \pm 0.3
	10	61.0 \pm 0.7	66.5 \pm 0.7	24.6 \pm 0.5	15.5 \pm 0.3
	25	60.8 \pm 0.6	66.4 \pm 0.6	18.4 \pm 0.3	13.1 \pm 0.2
	100	59.1 \pm 0.1	65.0 \pm 0.1	-	-

Table 3. **Evaluation of ECHO with sparse tracking.** We demonstrate versatility of ECHO input configuration by providing sparse tracking information along with ego-centric conditioning. Sparse information helps to improve the quality of prediction for modality with sparse tracking and regularize the other modality.

strates the effectiveness of our joint modeling formulation. For a fair comparison, all models were trained on the union of three datasets, with the exception of EgoAllo, for which we used the officially provided model trained on AMASS.

4.2. Sparse tracking

Egocentric human-object interactions are captured using different technologies and settings, often involving data streams (e.g., IMUs, head-mounted cameras) that provide further information, while often sparse. For example, while tracking objects from an egocentric camera remains an open challenge [2, 103], it is plausible that for a few frames, the location and orientation of the object can be determined by the camera view. We believe that such pieces of information provide important hints to reduce the uncertainty of the setting. ECHO is designed to take advantage of such an opportunity. We test its capability by simulating a scenario where one modality of the Human or the Object has a certain percentage of observed frames. Table 3 shows that additional constraints significantly improve the accuracy of the partially observed modality, while predictions for the fully unknown one show stability.

4.3. Ablation

We conduct an ablation study to analyze the effectiveness of several components of our method. All the models are trained in the same setting, except for the component that is being ablated. Firstly, we evaluate the model without inference time guidance (**NoGuide**), observing that it mostly affects the object prediction quality for the noisier data (i.e., BEHAVE). The evaluation results on BEHAVE are presented in Table 4, while results on OMOMO are presented in thew Sup.Mat.. We train the model without auxiliary

Method	BEHAVE			
	Human		Object	
	MPJPE↓	MPJVE↓	E_{v2v} ↓	E_c ↓
ECHO	61.4 \pm 1.0	66.8 \pm 1.1	29.5 \pm 0.9	17.1 \pm 0.7
NoGuide	61.2 \pm 1.1	66.6 \pm 1.1	29.8 \pm 0.9	17.5 \pm 0.7
NoAuxLoss	70.6 \pm 0.9	80.1 \pm 0.9	29.9 \pm 8.0	17.3 \pm 0.8
(\mathcal{H} , \mathcal{O})	72.1 \pm 3.0	80.4 \pm 3.2	33.0 \pm 1.9	21.0 \pm 1.3
NoAMASS	83.4 \pm 2.0	114.6 \pm 3.2	34.9 \pm 1.1	23.3 \pm 1.1
NoCan	125.0 \pm 9.8	172.1 \pm 15.8	39.5 \pm 4.6	28.0 \pm 4.1

Table 4. **Ablation study on BEHAVE.** Evaluating the impact of ECHO components proves the usefulness of guidance, our loss formulation, usage of three modalities, head-centric coordinate system, and training with AMASS data.

losses (**NoAuxLoss**) and observe that these losses mostly affect the quality of motion prediction, which is in line with our intuition, as two out of three losses are for human motion (joints and foot skating). The model without the interaction modality (i.e., working only with (\mathcal{H} , \mathcal{O})) has a substantially worse quality for both human and object motion predictions, suggesting that the contacts play a crucial role in connecting the other modalities within the model. Training the model without the AMASS dataset (**NoAMASS**) leads to an expected significant decrease in quality of human-motion modeling, highlighting the importance of large-scale datasets for learning the prior on human motion. Finally, we evaluate the effectiveness of our head-centric canonicalization of human and object motion, training the model that operates in world coordinates (**NoCan**).

5. Conclusions

In this work, we proposed ECHO the first model to predict Human-Object Interactions from just the tracking provided by sparse ego-centric sensors. We introduced a novel formulation that allows us to operate flexibly in different modalities, as well as a new conveyor inference that allows us to infer long temporal sequences. Our method solidly surpasses the state-of-the-art, producing high-quality predictions and providing a useful tool for downstream ego-centric settings.

Limitations and future work. As a first step in our novel formulation, we see a lot of yet unexplored potential. While we deal with HOI in isolation, incorporating conditioning coming from a surrounding scene would be instrumental to enable interaction in large environments (e.g., multi-floor scale). This could open to conditioning coming also from other sensors, like RGB cameras. We also explored interactions with objects of different natures and sizes, but interaction with tiny objects (e.g., pens, scissors) could require further sensors like haptic gloves, as fine motor interactions could have no effect on wrists and head sensors.

Acknowledgments Special thanks to Nikita Kister for the helpful discussions. We also thank RVH team for their help with proofreading the manuscript. This work is funded by the Deutsche Forschungsgemeinschaft - 409792180 (EmmyNoether Programme, project: Real Virtual Humans) and the German Federal Ministry of Education and Research (BMBF): Tübingen AI Center, FKZ: 01IS18039A. G. Pons-Moll is a member of the Machine Learning Cluster of Excellence, EXC number 2064/1 – Project number 390727645. The authors thank the International Max Planck Research School for Intelligent Systems (IMPRS-IS) for supporting I. A. Petrov. R. Marin has been supported by the European Union’s Horizon 2020 research and innovation program under the Marie Skłodowska-Curie grant agreement No 101109330. The project was made possible by funding from the Carl Zeiss Foundation. The computational resources for this project were provided by the Google Cloud grant.

References

- [1] Hiroyasu Akada, Jian Wang, Soshi Shimada, Masaki Takahashi, Christian Theobalt, and Vladislav Golyanik. Unrealego: A new dataset for robust egocentric 3d human motion capture. In *European Conference on Computer Vision*, pages 1–17. Springer, 2022. 2
- [2] Prithviraj Banerjee, Sindi Shkodrani, Pierre Moulon, Shreyas Hampali, Fan Zhang, Jade Fountain, Edward Miller, Selen Basol, Richard Newcombe, Robert Wang, et al. Introducing hot3d: An egocentric dataset for 3d hand and object tracking. *arXiv preprint arXiv:2406.09598*, 2024. 8
- [3] Fan Bao, Shen Nie, Kaiwen Xue, Chongxuan Li, Shi Pu, Yaole Wang, Gang Yue, Yue Cao, Hang Su, and Jun Zhu. One transformer fits all distributions in multi-modal diffusion at scale. In *Proceedings of the 40th International Conference on Machine Learning*. JMLR.org, 2023. 4
- [4] German Barquero, Nadine Bertsch, Manojkumar Marramreddy, Carlos Chacón, Filippo Arcadu, Ferran Rigual, Nicky Sijia He, Cristina Palmero, Sergio Escalera, Yuting Ye, et al. From sparse signal to smooth motion: Real-time motion generation with rolling prediction models. In *Proceedings of the Computer Vision and Pattern Recognition Conference*, pages 1850–1860, 2025. 2
- [5] Bharat Lal Bhatnagar, Suriya Singh, Chetan Arora, and C.V. Jawahar. Unsupervised learning of deep feature representation for clustering egocentric actions. In *Proceedings of the Twenty-Sixth International Joint Conference on Artificial Intelligence, IJCAI-17*, pages 1447–1453, 2017. 2
- [6] Bharat Lal Bhatnagar, Xianghui Xie, Ilya A Petrov, Cristian Sminchisescu, Christian Theobalt, and Gerard Pons-Moll. Behave: Dataset and method for tracking human object interactions. In *Proceedings of the IEEE/CVF Conference on Computer Vision and Pattern Recognition*, pages 15935–15946, 2022. 3, 6
- [7] Jona Braun, Sammy Christen, Muhammed Kocabas, Emre Aksan, and Otmar Hilliges. Physically plausible full-body hand-object interaction synthesis. In *2024 International Conference on 3D Vision (3DV)*, pages 464–473. IEEE, 2024. 3
- [8] Congqi Cao, Yifan Zhang, Yi Wu, Hanqing Lu, and Jian Cheng. Egocentric gesture recognition using recurrent 3d convolutional neural networks with spatiotemporal transformer modules. *2017 IEEE International Conference on Computer Vision (ICCV)*, 2017. 2
- [9] Yukang Cao, Liang Pan, Kai Han, Kwan-Yee K Wong, and Ziwei Liu. Avatargo: Zero-shot 4d human-object interaction generation and animation. *arXiv preprint arXiv:2410.07164*, 2024. 3
- [10] Angela Castillo, Maria Escobar, Guillaume Jeanneret, Albert Pumarola, Pablo Arbeláez, Ali Thabet, and Artsiom Sanakoyeu. Bodiffusion: Diffusing sparse observations for full-body human motion synthesis. In *Proceedings of the IEEE/CVF International Conference on Computer Vision*, pages 4221–4231, 2023. 2, 3, 4, 5, 7
- [11] Boyuan Chen, Diego Martí Monsó, Yilun Du, Max Simchowitz, Russ Tedrake, and Vincent Sitzmann. Diffusion forcing: Next-token prediction meets full-sequence diffusion. *Advances in Neural Information Processing Systems*, 37:24081–24125, 2024. 5
- [12] Mia Chiquier and Carl Vondrick. Muscles in action. In *Proceedings of the IEEE/CVF International Conference on Computer Vision*, pages 22091–22101, 2023. 2
- [13] Peng Dai, Yang Zhang, Tao Liu, Zhen Fan, Tianyuan Du, Zhuo Su, Xiaozheng Zheng, and Zeming Li. Hmd-poser: On-device real-time human motion tracking from scalable sparse observations. In *Proceedings of the IEEE/CVF Conference on Computer Vision and Pattern Recognition*, pages 874–884, 2024. 2
- [14] Sisi Dai, Wenhao Li, Haowen Sun, Haibin Huang, Chongyang Ma, Hui Huang, Kai Xu, and Ruizhen Hu. Interfusion: Text-driven generation of 3d human-object interaction. In *European Conference on Computer Vision*, pages 18–35. Springer, 2024. 3
- [15] Yudi Dai, Yitai Lin, Chenglu Wen, Siqi Shen, Lan Xu, Jingyi Yu, Yuexin Ma, and Cheng Wang. Hsc4d: Human-centered 4d scene capture in large-scale indoor-outdoor space using wearable imus and lidar. In *Proceedings of the IEEE/CVF Conference on Computer Vision and Pattern Recognition*, pages 6792–6802, 2022. 2, 3
- [16] Prafulla Dhariwal and Alexander Nichol. Diffusion models beat gans on image synthesis. *Advances in neural information processing systems*, 34:8780–8794, 2021. 6
- [17] Christian Diller and Angela Dai. Cg-hoi: Contact-guided 3d human-object interaction generation. In *Proceedings of the IEEE/CVF Conference on Computer Vision and Pattern Recognition*, pages 19888–19901, 2024. 3
- [18] Yuming Du, Robin Kips, Albert Pumarola, Sebastian Starke, Ali Thabet, and Artsiom Sanakoyeu. Avatars grow legs: Generating smooth human motion from sparse tracking inputs with diffusion model. In *Proceedings of the IEEE/CVF Conference on Computer Vision and Pattern Recognition*, pages 481–490, 2023. 2
- [19] Maria Escobar, Juanita Puentes, Cristhian Forigua, Jordi Pont-Tuset, Kevis-Kokitsi Maninis, and Pablo Arbeláez.

- Egocast: Forecasting egocentric human pose in the wild. In *2025 IEEE/CVF Winter Conference on Applications of Computer Vision (WACV)*, pages 5831–5841. IEEE, 2025. 2
- [20] Zicong Fan, Omid Taheri, Dimitrios Tzionas, Muhammed Kocabas, Manuel Kaufmann, Michael J Black, and Otmar Hilliges. Arctic: A dataset for dexterous bimanual hand-object manipulation. In *Proceedings of the IEEE/CVF Conference on Computer Vision and Pattern Recognition*, pages 12943–12954, 2023. 3
- [21] Alireza Fathi, Ali Farhadi, and James M Rehg. Understanding egocentric activities. In *2011 international conference on computer vision*, pages 407–414. IEEE, 2011. 2
- [22] Ruili Feng, Han Zhang, Zhantao Yang, Jie Xiao, Zhilei Shu, Zhiheng Liu, Andy Zheng, Yukun Huang, Yu Liu, and Hongyang Zhang. The matrix: Infinite-horizon world generation with real-time moving control. *arXiv preprint arXiv:2412.03568*, 2024. 5
- [23] Anindita Ghosh, Rishabh Dabral, Vladislav Golyanik, Christian Theobalt, and Philipp Slusallek. Imos: Intent-driven full-body motion synthesis for human-object interactions. In *Computer Graphics Forum*, pages 1–12. Wiley Online Library, 2023. 3
- [24] Vladimir Guzov, Aymen Mir, Torsten Sattler, and Gerard Pons-Moll. Human poseitioning system (hps): 3d human pose estimation and self-localization in large scenes from body-mounted sensors. In *IEEE Conference on Computer Vision and Pattern Recognition (CVPR)*. IEEE, 2021. 2, 3
- [25] Vladimir Guzov, Julian Chibane, Riccardo Marin, Yannan He, Yunus Saracoglu, Torsten Sattler, and Gerard Pons-Moll. Interaction replica: Tracking human-object interaction and scene changes from human motion. In *International Conference on 3D Vision (3DV)*, 2024. 2, 3
- [26] Vladimir Guzov, Ilya A Petrov, and Gerard Pons-Moll. Blendify – python rendering framework for blender. *arXiv preprint arXiv:2410.17858*, 2024. 6
- [27] Vladimir Guzov, Yifeng Jiang, Fangzhou Hong, Gerard Pons-Moll, Richard Newcombe, C. Karen Liu, Yuting Ye, and Lingni Ma. Hmd²: Environment-aware motion generation from single egocentric head-mounted device. In *International Conference on 3D Vision (3DV)*, 2025. 2, 3, 5
- [28] Mohamed Hassan, Vasileios Choutas, Dimitrios Tzionas, and Michael J Black. Resolving 3d human pose ambiguities with 3d scene constraints. In *Proceedings of the IEEE/CVF international conference on computer vision*, pages 2282–2292, 2019. 3
- [29] Mohamed Hassan, Partha Ghosh, Joachim Tesch, Dimitrios Tzionas, and Michael J Black. Populating 3d scenes by learning human-scene interaction. In *Proceedings of the IEEE/CVF Conference on Computer Vision and Pattern Recognition*, pages 14708–14718, 2021. 3
- [30] Jonathan Ho, Ajay Jain, and Pieter Abbeel. Denoising diffusion probabilistic models. *Advances in neural information processing systems*, 33:6840–6851, 2020. 4, 1
- [31] Dominik Hollidt, Paul Streli, Jiayi Jiang, Yasaman Haghighi, Changlin Qian, Xintong Liu, and Christian Holz. Egosim: An egocentric multi-view simulator and real dataset for body-worn cameras during motion and activity. *Advances in Neural Information Processing Systems*, 37: 106607–106627, 2024. 2
- [32] HoloLens. Microsoft HoloLens, accessed January 7, 2025. <https://learn.microsoft.com/en-us/hololens/>. 2
- [33] Siyuan Huang, Zan Wang, Puhao Li, Baoxiong Jia, Tengyu Liu, Yixin Zhu, Wei Liang, and Song-Chun Zhu. Diffusion-based generation, optimization, and planning in 3d scenes. In *Proceedings of the IEEE/CVF Conference on Computer Vision and Pattern Recognition*, pages 16750–16761, 2023. 3
- [34] Yinghao Huang, Manuel Kaufmann, Emre Aksan, Michael J. Black, Otmar Hilliges, and Gerard Pons-Moll. Deep inertial poser: Learning to reconstruct human pose from sparse inertial measurements in real time. *ACM Transactions on Graphics, (Proc. SIGGRAPH Asia)*, 37(6): 185:1–185:15, 2018. 2
- [35] Yinghao Huang, Omid Taheri, Michael J. Black, and Dimitrios Tzionas. InterCap: Joint markerless 3D tracking of humans and objects in interaction from multi-view RGB-D images. *International Journal of Computer Vision (IJCV)*, 2024. 3
- [36] Jiayi Jiang, Paul Streli, Huajian Qiu, Andreas Fender, Larissa Laich, Patrick Snape, and Christian Holz. Avatarposer: Articulated full-body pose tracking from sparse motion sensing. In *European conference on computer vision*, pages 443–460. Springer, 2022. 2
- [37] Nan Jiang, Zhiyuan Zhang, Hongjie Li, Xiaoxuan Ma, Zan Wang, Yixin Chen, Tengyu Liu, Yixin Zhu, and Siyuan Huang. Scaling up dynamic human-scene interaction modeling. In *Proceedings of the IEEE/CVF Conference on Computer Vision and Pattern Recognition*, pages 1737–1747, 2024. 3
- [38] Yuheng Jiang, Suyi Jiang, Guoxing Sun, Zhuo Su, Kaiwen Guo, Minye Wu, Jingyi Yu, and Lan Xu. Neuralhofusion: Neural volumetric rendering under human-object interactions. In *Proceedings of the IEEE/CVF Conference on Computer Vision and Pattern Recognition*, pages 6155–6165, 2022. 3
- [39] Yifeng Jiang, Yuting Ye, Deepak Gopinath, Jungdam Won, Alexander W Winkler, and C Karen Liu. Transformer inertial poser: Real-time human motion reconstruction from sparse imus with simultaneous terrain generation. In *SIGGRAPH Asia 2022 Conference Papers*, pages 1–9, 2022. 2
- [40] Taeho Kang, Kyungjin Lee, Jinrui Zhang, and Youngki Lee. Ego3dpose: Capturing 3d cues from binocular egocentric views. In *SIGGRAPH Asia 2023 Conference Papers*, pages 1–10, 2023. 2
- [41] Manuel Kaufmann, Yi Zhao, Chengcheng Tang, Lingling Tao, Christopher Twigg, Jie Song, Robert Wang, and Otmar Hilliges. Em-pose: 3d human pose estimation from sparse electromagnetic trackers. In *Proceedings of the IEEE/CVF international conference on computer vision*, pages 11510–11520, 2021. 2
- [42] Manuel Kaufmann, Velko Vechev, and Dario Mylonopoulos. aitviewer, 2022. 6
- [43] Nilesh Kulkarni, Davis Rempe, Kyle Genova, Abhijit Kundu, Justin Johnson, David Fouhey, and Leonidas

- Guibas. Nifty: Neural object interaction fields for guided human motion synthesis. In *Proceedings of the IEEE/CVF Conference on Computer Vision and Pattern Recognition*, pages 947–957, 2024. 3
- [44] Jiye Lee and Hanbyul Joo. Mocap everyone everywhere: Lightweight motion capture with smartwatches and a head-mounted camera. In *Proceedings of the IEEE/CVF conference on computer vision and pattern recognition*, pages 1091–1100, 2024. 2, 3
- [45] Jihyun Lee, Weipeng Xu, Alexander Richard, Shih-En Wei, Shunsuke Saito, Shaojie Bai, Te-Li Wang, Minhyuk Sung, Jason Saragih, et al. Rewind: Real-time egocentric whole-body motion diffusion with exemplar-based identity conditioning. *arXiv preprint arXiv:2504.04956*, 2025. 2
- [46] Jiaman Li, Karen Liu, and Jiajun Wu. Ego-body pose estimation via ego-head pose estimation. In *Proceedings of the IEEE/CVF Conference on Computer Vision and Pattern Recognition*, pages 17142–17151, 2023. 2, 7
- [47] Jiaman Li, Jiajun Wu, and C Karen Liu. Object motion guided human motion synthesis. *ACM Transactions on Graphics (TOG)*, 42(6):1–11, 2023. 3, 6
- [48] Jiaman Li, Alexander Clegg, Roozbeh Mottaghi, Jiajun Wu, Xavier Puig, and C Karen Liu. Controllable human-object interaction synthesis. In *European Conference on Computer Vision*, pages 54–72. Springer, 2024. 3
- [49] Quanzhou Li, Jingbo Wang, Chen Change Loy, and Bo Dai. Task-oriented human-object interactions generation with implicit neural representations. In *Proceedings of the IEEE/CVF Winter Conference on Applications of Computer Vision*, pages 3035–3044, 2024. 3
- [50] Bonan Liu, Handi Yin, Manuel Kaufmann, Jinhao He, Sammy Christen, Jie Song, and Pan Hui. EgoHdm: An online egocentric-inertial human motion capture, localization, and dense mapping system. *arXiv preprint arXiv:2409.00343*, 2024. 2, 3
- [51] Yuxuan Liu, Jianxin Yang, Xiao Gu, Yijun Chen, Yao Guo, and Guang-Zhong Yang. Egofish3d: Egocentric 3d pose estimation from a fisheye camera via self-supervised learning. *IEEE Transactions on Multimedia*, 25:8880–8891, 2023. 2
- [52] Yuxuan Liu, Jianxin Yang, Xiao Gu, Yao Guo, and Guang-Zhong Yang. Egohmr: Egocentric human mesh recovery via hierarchical latent diffusion model. In *2023 IEEE International Conference on Robotics and Automation (ICRA)*, pages 9807–9813. IEEE, 2023. 2
- [53] Ilya Loshchilov and Frank Hutter. Decoupled weight decay regularization. *arXiv preprint arXiv:1711.05101*, 2017. 6
- [54] Lingni Ma, Yuting Ye, Fangzhou Hong, Vladimir Guzov, Yifeng Jiang, Rowan Postyeni, Luis Pesqueira, Alexander Gamino, Vijay Baiyya, Hyo Jin Kim, et al. Nymeria: A massive collection of multimodal egocentric daily motion in the wild. In *European Conference on Computer Vision*, pages 445–465. Springer, 2024. 2
- [55] Minghuang Ma, Haoqi Fan, and Kris M Kitani. Going deeper into first-person activity recognition. In *Proceedings of the IEEE Conference on Computer Vision and Pattern Recognition*, pages 1894–1903, 2016. 2
- [56] Naureen Mahmood, Nima Ghorbani, Nikolaus F. Troje, Gerard Pons-Moll, and Michael J. Black. AMASS: Archive of motion capture as surface shapes. In *International Conference on Computer Vision*, pages 5442–5451, 2019. 5, 6
- [57] Aymen Mir, Xavier Puig, Angjoo Kanazawa, and Gerard Pons-Moll. Generating continual human motion in diverse 3d scenes. In *2024 International Conference on 3D Vision (3DV)*, pages 903–913. IEEE, 2024. 3
- [58] Vimal Molyn, Riku Arakawa, Mayank Goel, Chris Harrison, and Karan Ahuja. Imuposer: Full-body pose estimation using imus in phones, watches, and earbuds. In *Proceedings of the 2023 CHI Conference on Human Factors in Computing Systems*, pages 1–12, 2023. 2
- [59] Hyeongjin Nam, Daniel Sungho Jung, Gyeongsik Moon, and Kyoung Mu Lee. Joint reconstruction of 3d human and object via contact-based refinement transformer. In *Proceedings of the IEEE/CVF Conference on Computer Vision and Pattern Recognition*, pages 10218–10227, 2024. 3
- [60] Georgios Pavlakos, Vasileios Choutas, Nima Ghorbani, Timo Bolkart, Ahmed A. A. Osman, Dimitrios Tzionas, and Michael J. Black. Expressive body capture: 3D hands, face, and body from a single image. In *Proceedings IEEE Conf. on Computer Vision and Pattern Recognition (CVPR)*, pages 10975–10985, 2019. 4
- [61] William Peebles and Saining Xie. Scalable diffusion models with transformers. In *Proceedings of the IEEE/CVF international conference on computer vision*, pages 4195–4205, 2023. 5, 7
- [62] Xiaogang Peng, Yiming Xie, Zizhao Wu, Varun Jampani, Deqing Sun, and Huaizu Jiang. Hoi-diff: Text-driven synthesis of 3d human-object interactions using diffusion models. *arXiv preprint arXiv:2312.06553*, 2023. 3
- [63] Ilya A Petrov, Riccardo Marin, Julian Chibane, and Gerard Pons-Moll. Object pop-up: Can we infer 3d objects and their poses from human interactions alone? In *Proceedings of the IEEE/CVF Conference on Computer Vision and Pattern Recognition*, 2023. 3, 7
- [64] Ilya A Petrov, Riccardo Marin, Julian Chibane, and Gerard Pons-Moll. Tridi: Trilateral diffusion of 3d humans, objects, and interactions. In *Proceedings of the IEEE/CVF International Conference on Computer Vision*, 2025. 3, 4
- [65] Project Aria. *Project Aria*, accessed January 7, 2025. <https://www.projectaria.com/>. 2
- [66] Project Aria Machine Perception Services. Project aria machine perception services, accessed January 7, 2025. 2
- [67] Guocheng Qian, Yuchen Li, Houwen Peng, Jinjie Mai, Hasan Hammoud, Mohamed Elhoseiny, and Bernard Ghanem. Pointnext: Revisiting pointnet++ with improved training and scaling strategies. *Advances in neural information processing systems*, 35:23192–23204, 2022. 4
- [68] Aditya Ramesh, Prafulla Dhariwal, Alex Nichol, Casey Chu, and Mark Chen. Hierarchical text-conditional image generation with clip latents. *arXiv preprint arXiv:2204.06125*, 1(2):3, 2022. 4, 1
- [69] Helge Rhodin, Christian Richardt, Dan Casas, Eldar Insafutdinov, Mohammad Shafiei, Hans-Peter Seidel, Bernt Schiele, and Christian Theobalt. Egocap: egocentric marker-less motion capture with two fisheye cameras. *ACM Transactions on Graphics (TOG)*, 35(6):1–11, 2016. 2

- [70] Grégory Rogez, James S Supancic, and Deva Ramanan. First-person pose recognition using egocentric workspaces. In *Proceedings of the IEEE conference on computer vision and pattern recognition*, pages 4325–4333, 2015. 2
- [71] Javier Romero, Dimitrios Tzionas, and Michael J. Black. Embodied hands: Modeling and capturing hands and bodies together. *ACM Transactions on Graphics, (Proc. SIGGRAPH Asia)*, 36(6), 2017. 6
- [72] Jascha Sohl-Dickstein, Eric Weiss, Niru Maheswaranathan, and Surya Ganguli. Deep unsupervised learning using nonequilibrium thermodynamics. In *International conference on machine learning*, pages 2256–2265. PMLR, 2015. 4
- [73] Wenfeng Song, Xinyu Zhang, Shuai Li, Yang Gao, Aimin Hao, Xia Hou, Chenglizhao Chen, Ning Li, and Hong Qin. Hoianimator: Generating text-prompt human-object animations using novel perceptive diffusion models. In *Proceedings of the IEEE/CVF Conference on Computer Vision and Pattern Recognition*, pages 811–820, 2024. 3
- [74] István Sárándi and Gerard Pons-Moll. Neural localizer fields for continuous 3d human pose and shape estimation. *Advances in Neural Information Processing Systems (NeurIPS)*, 2024. 6
- [75] Jiangnan Tang, Jingya Wang, Kaiyang Ji, Lan Xu, Jingyi Yu, and Ye Shi. A unified diffusion framework for scene-aware human motion estimation from sparse signals. In *Proceedings of the IEEE/CVF Conference on Computer Vision and Pattern Recognition*, pages 21251–21262, 2024. 3
- [76] Guy Tevet, Sigal Raab, Brian Gordon, Yonatan Shafir, Daniel Cohen-Or, and Amit H Bermano. Human motion diffusion model. *arXiv preprint arXiv:2209.14916*, 2022. 5
- [77] Denis Tome, Thiemo Alldieck, Patrick Peluse, Gerard Pons-Moll, Lourdes Agapito, Hernan Badino, and Fernando De la Torre. Selfpose: 3d egocentric pose estimation from a headset mounted camera. *IEEE Transactions on Pattern Analysis and Machine Intelligence*, 45(6):6794–6806, 2020. 2
- [78] Shashank Tripathi, Agniv Chatterjee, Jean-Claude Passy, Hongwei Yi, Dimitrios Tzionas, and Michael J Black. Deco: Dense estimation of 3d human-scene contact in the wild. In *Proceedings of the IEEE/CVF International Conference on Computer Vision*, pages 8001–8013, 2023. 3
- [79] Daniel Vlasic, Rolf Adelsberger, Giovanni Vannucci, John Barnwell, Markus Gross, Wojciech Matusik, and Jovan Popović. Practical motion capture in everyday surroundings. *ACM transactions on graphics (TOG)*, 26(3):35–es, 2007. 2
- [80] Timo Von Marcard, Bodo Rosenhahn, Michael J Black, and Gerard Pons-Moll. Sparse inertial poser: Automatic 3d human pose estimation from sparse imus. In *Computer graphics forum*, pages 349–360. Wiley Online Library, 2017. 2
- [81] Jian Wang, Zhe Cao, Diogo Luvizon, Lingjie Liu, Kripasindhu Sarkar, Danhang Tang, Thabo Beeler, and Christian Theobalt. Egocentric whole-body motion capture with fisheyeit and diffusion-based motion refinement. In *Proceedings of the IEEE/CVF Conference on Computer Vision and Pattern Recognition*, pages 777–787, 2024. 2
- [82] Alexander Winkler, Jungdam Won, and Yuting Ye. Questsim: Human motion tracking from sparse sensors with simulated avatars. In *SIGGRAPH Asia 2022 Conference Papers*, pages 1–8, 2022. 2
- [83] Xianghui Xie, Bharat Lal Bhatnagar, and Gerard Pons-Moll. Chore: Contact, human and object reconstruction from a single rgb image. In *European Conference on Computer Vision (ECCV)*. Springer, 2022. 3
- [84] Xianghui Xie, Bharat Lal Bhatnagar, and Gerard Pons-Moll. Visibility aware human-object interaction tracking from single rgb camera. In *IEEE Conference on Computer Vision and Pattern Recognition (CVPR)*, 2023.
- [85] Xianghui Xie, Bharat Lal Bhatnagar, Jan Eric Lenssen, and Gerard Pons-Moll. Template free reconstruction of human-object interaction with procedural interaction generation. In *Proceedings of the IEEE/CVF Conference on Computer Vision and Pattern Recognition*, pages 10003–10015, 2024.
- [86] Xianghui Xie, Jan Eric Lenssen, and Gerard Pons-Moll. Intertrack: Tracking human object interaction without object templates. In *International Conference on 3D Vision 2025*, 2025. 3
- [87] Liang Xu, Yizhou Zhou, Yichao Yan, Xin Jin, Wenhan Zhu, Fengyun Rao, Xiaokang Yang, and Wenjun Zeng. Regenet: Towards human action-reaction synthesis. In *Proceedings of the IEEE/CVF Conference on Computer Vision and Pattern Recognition*, pages 1759–1769, 2024. 3
- [88] Sirui Xu, Zhengyuan Li, Yu-Xiong Wang, and Liang-Yan Gui. Interdiff: Generating 3d human-object interactions with physics-informed diffusion. In *Proceedings of the IEEE/CVF International Conference on Computer Vision*, pages 14928–14940, 2023. 3, 7
- [89] Sirui Xu, Yu-Xiong Wang, Liangyan Gui, et al. Interdreamer: Zero-shot text to 3d dynamic human-object interaction. *Advances in Neural Information Processing Systems*, 37:52858–52890, 2024. 3
- [90] Vasco Xu, Chenfeng Gao, Henry Hoffmann, and Karan Ahuja. Mobileposer: Real-time full-body pose estimation and 3d human translation from imus in mobile consumer devices. In *Proceedings of the 37th Annual ACM Symposium on User Interface Software and Technology*, pages 1–11, 2024. 2
- [91] Weipeng Xu, Avishek Chatterjee, Michael Zollhoefer, Helge Rhodin, Pascal Fua, Hans-Peter Seidel, and Christian Theobalt. Mo²Cap²: Real-time mobile 3d motion capture with a cap-mounted fisheye camera. *IEEE Transactions on Visualization and Computer Graphics*, pages 1–1, 2019. 2
- [92] Jie Yang, Xuesong Niu, Nan Jiang, Ruimao Zhang, and Siyuan Huang. F-hoi: Toward fine-grained semantic-aligned 3d human-object interactions. In *European Conference on Computer Vision*, pages 91–110. Springer, 2024. 3
- [93] Yuhang Yang, Wei Zhai, Chengfeng Wang, Chengjun Yu, Yang Cao, and Zheng-Jun Zha. Egochoir: Capturing 3d human-object interaction regions from egocentric views. *Advances in Neural Information Processing Systems*, 37: 54529–54557, 2024. 2
- [94] Brent Yi, Vickie Ye, Maya Zheng, Yunqi Li, Lea Müller, Georgios Pavlakos, Yi Ma, Jitendra Malik, and Angjoo

- Kanazawa. Estimating body and hand motion in an ego-sensed world. *arXiv preprint arXiv:2410.03665*, 2024. 2, 3, 5, 6, 7
- [95] Xinyu Yi, Yuxiao Zhou, and Feng Xu. Transpose: Real-time 3d human translation and pose estimation with six inertial sensors. *ACM Transactions On Graphics (TOG)*, 40(4):1–13, 2021. 2
- [96] Xinyu Yi, Yuxiao Zhou, Marc Habermann, Soshi Shimada, Vladislav Golyanik, Christian Theobalt, and Feng Xu. Physical inertial poser (pip): Physics-aware real-time human motion tracking from sparse inertial sensors. In *Proceedings of the IEEE/CVF conference on computer vision and pattern recognition*, pages 13167–13178, 2022. 2
- [97] H. Yonemoto, K. Murasaki, T. Osawa, K. Sudo, J. Shimamura, and Y. Taniguchi. Egocentric articulated pose tracking for action recognition. In *International Conference on Machine Vision Applications (MVA)*, 2015. 2
- [98] Juze Zhang, Haimin Luo, Hongdi Yang, Xinru Xu, Qianyang Wu, Ye Shi, Jingyi Yu, Lan Xu, and Jingya Wang. Neurdome: A neural modeling pipeline on multi-view human-object interactions. In *Proceedings of the IEEE/CVF Conference on Computer Vision and Pattern Recognition*, pages 8834–8845, 2023. 3
- [99] Juze Zhang, Jingyan Zhang, Zining Song, Zhanhe Shi, Chengfeng Zhao, Ye Shi, Jingyi Yu, Lan Xu, and Jingya Wang. Hoi-m³: Capture multiple humans and objects interaction within contextual environment. In *Proceedings of the IEEE/CVF Conference on Computer Vision and Pattern Recognition*, pages 516–526, 2024. 3
- [100] Siwei Zhang, Qianli Ma, Yan Zhang, Zhiyin Qian, Taein Kwon, Marc Pollefeys, Federica Bogo, and Siyu Tang. Egobody: Human body shape and motion of interacting people from head-mounted devices. In *European conference on computer vision*, pages 180–200. Springer, 2022. 2
- [101] Xiaohan Zhang, Bharat Lal Bhatnagar, Sebastian Starke, Ilya Petrov, Vladimir Guзов, Helisa Dhamo, Eduardo Pérez-Pellitero, and Gerard Pons-Moll. Force: Physics-aware human-object interaction. *arXiv preprint arXiv:2403.11237*, 2024. 3
- [102] Xiaohan Zhang, Sebastian Starke, Vladimir Guзов, Zhensong Zhang, Eduardo Pérez Pellitero, and Gerard Pons-Moll. Scenic: Scene-aware semantic navigation with instruction-guided control. *arXiv preprint arXiv:2412.15664*, 2024. 3
- [103] Yunhan Zhao, Haoyu Ma, Shu Kong, and Charless Fowlkes. Instance tracking in 3d scenes from egocentric videos. In *Proceedings of the IEEE/CVF Conference on Computer Vision and Pattern Recognition*, pages 21933–21944, 2024. 8
- [104] Xiaozheng Zheng, Zhuo Su, Chao Wen, Zhou Xue, and Xiaojie Jin. Realistic full-body tracking from sparse observations via joint-level modeling. In *Proceedings of the IEEE/CVF International Conference on Computer Vision*, pages 14678–14688, 2023. 2, 7
- [105] Yi Zhou, Connelly Barnes, Jingwan Lu, Jimei Yang, and Hao Li. On the continuity of rotation representations in neural networks. In *Proceedings of the IEEE/CVF conference on computer vision and pattern recognition*, pages 5745–5753, 2019. 4
- [106] Chengxu Zuo, Yiming Wang, Lishuang Zhan, Shihui Guo, Xinyu Yi, Feng Xu, and Yipeng Qin. Loose inertial poser: Motion capture with imu-attached loose-wear jacket. In *Proceedings of the IEEE/CVF Conference on Computer Vision and Pattern Recognition*, pages 2209–2219, 2024. 2

ECHO: Ego-Centric modeling of Human-Object interactions

Supplementary Material

Symbol	Description	Domain
W	Network’s temporal window	60 frames
N	Input sequence length	\mathbb{N}
\mathcal{E}	3 point ego-centric conditioning	$\left\{ \begin{bmatrix} \mathbf{R}_{3p}, \boldsymbol{\omega}_{3p}, \\ J_{3p}, \mathbf{v}_{3p} \end{bmatrix}^{1..N} \right\}$
\mathbf{R}_{3p}	Rotation of 3 p. cond.	\mathbb{R}^{18}
$\boldsymbol{\omega}_{3p}$	Rotation velocity of 3 p. cond.	\mathbb{R}^{18}
J_{3p}	XYZ coordinates of 3 p. cond.	\mathbb{R}^9
\mathbf{v}_{3p}	Coordinate velocity of 3 p. cond.	\mathbb{R}^9
\mathcal{H}	Human Modality	$\{\mathbf{T}_{\mathcal{H}}, \boldsymbol{\theta}_{\mathcal{H}}\}^{1..N}$
$\boldsymbol{\theta}_{\mathcal{H}}$	Human Pose	$\mathbb{R}^{51 \times 3}$
β	Human Shape parameters	\mathbb{R}^{10}
$\mathbf{V}_{\mathcal{H}}$	Human Template’s Vertices	\mathbb{R}^{10475}
$\mathbf{T}_{\mathcal{H}}$	Human Global (R, t) transformation	\mathbb{R}^9
\mathcal{O}	Object Modality	$\{\mathbf{T}_{\mathcal{O}}\}^{1..N}$
$\mathbf{T}_{\mathcal{O}}$	Object Global (R, t) transformation	\mathbb{R}^9
$\mathcal{C}_{\mathcal{O}}$	Object Information for conditioning	$(\mathbf{f}_{\mathcal{O}}, \mathbf{y}_{\mathcal{O}})$
$\mathbf{f}_{\mathcal{O}}$	PointNext features object	\mathbb{R}^{1024}
$\mathbf{y}_{\mathcal{O}}$	one-hot encoding of the class	$\{0, 1\}^{33}$
$\mathbf{V}_{\mathcal{O}}$	Object Template’s Vertices	\mathbb{R}^{1500}
\mathcal{I}	Interaction	$\mathcal{I} = \{c_{\mathcal{I}}\}^{1..N}$
$c_{\mathcal{I}}$	Vector of contact labels	$\{0, 1\}^{68}$
\mathbf{P}_c	Contact points on the human body	\mathbb{R}^{64}

Table S1. **Notation Table.** The main notation used in our paper.

6. Broader impacts

The ability of our model to capture and generate continuous human-object interactions offers significant value for fields such as digital content creation and ergonomics. This research direction could enable new applications for studying human behavior and developing realistic virtual experiences. However, this technology can also be misused. Tracking detailed human actions could lead to unauthorized surveillance, creating privacy issues. We recognize that future advances might make this technology easier to abuse. Therefore, we believe that its responsible development must be an ongoing priority.

7. Background and Notation

Background. The forward diffusion process can be formulated as a Markov chain with T steps. Starting from a clean sample \mathbf{z}_0 it produces a series of distributions $q(\mathbf{z}_t|\mathbf{z}_{t-1})$: $q(\mathbf{z}_{1:T}|\mathbf{z}_0) = \prod_{t=1}^T q(\mathbf{z}_t|\mathbf{z}_{t-1})$. We add noise to the distribution for T steps, until finally \mathbf{z}_T becomes a sample from $\mathcal{N}(\mathbf{0}, \mathbf{I})$. Defining $\beta_0 = 0$, and $\beta_t \in (0, 1)$ we obtain:

$$q(\mathbf{z}_t|\mathbf{z}_{t-1}) = \mathcal{N}(\mathbf{z}_t; \sqrt{1 - \beta_t}\mathbf{z}_{t-1}, \beta_t\mathbf{I}). \quad (8)$$

Formulation of DDPM [30] allows us to obtain a closed-

Mode	BEHAVE			
	Human		Object	
	MPJPE↓	MPJVE↓	$E_{v2v} \downarrow$	$E_c \downarrow$
ECHO	61.4 \pm 1.0	66.8 \pm 1.1	29.5 \pm 0.9	17.1 \pm 0.7
ECHO w. \mathcal{H}	-	-	28.0 \pm 0.1	16.1 \pm 0.1
ECHO w. \mathcal{O}	59.1 \pm 0.1	65.0 \pm 0.1	-	-
ECHO w. \mathcal{I}	59.0 \pm 0.7	65.1 \pm 0.8	27.0 \pm 0.8	14.2 \pm 0.3

Table S2. **Evaluation of ECHO with additional input modalities.** We observe that providing ECHO with contacts information provides the biggest quality improvement among all three modalities.

Method	OMOMO			
	Human		Object	
	MPJPE↓	MPJVE↓	$E_{v2v} \downarrow$	$E_c \downarrow$
ECHO	64.1\pm2.9	69.7 \pm 3.2	26.7 \pm 1.9	15.6 \pm 1.1
NoGuide	64.5 \pm 3.0	69.4\pm3.1	26.5\pm2.1	15.4\pm1.2
NoAuxLoss	69.7 \pm 3.2	82.9 \pm 3.8	27.5 \pm 2.7	16.7 \pm 1.1
(\mathcal{H}, \mathcal{O})	82.5 \pm 4.9	93.1 \pm 5.5	30.0 \pm 4.4	18.7 \pm 1.8
NoAMASS	85.2 \pm 2.2	121.3 \pm 3.6	28.7 \pm 1.8	18.1 \pm 0.9
NoCan	125.7 \pm 9.1	181.3 \pm 17.9	34.6 \pm 4.4	23.8 \pm 3.1

Table S3. **Ablation study on OMOMO.** Evaluating the impact of ECHO components proves the usefulness of guidance, our loss formulation, usage of three modalities, head-centric coord. system, and training with AMASS data.

form expression for \mathbf{z}_t . Let $\alpha_i = 1 - \beta_i$, $\bar{\alpha}_t = \prod_{i=1}^t \alpha_i$, and $\epsilon \in \mathcal{N}(\mathbf{0}, \mathbf{I})$:

$$\begin{aligned} q(\mathbf{z}_t|\mathbf{z}_0) &= \mathcal{N}(\mathbf{z}_t; \sqrt{\bar{\alpha}_t}\mathbf{z}_0, (1 - \bar{\alpha}_t)\mathbf{I}), \\ \mathbf{z}_t &= \sqrt{\bar{\alpha}_t}\mathbf{z}_0 + \sqrt{1 - \bar{\alpha}_t}\epsilon. \end{aligned} \quad (9)$$

Reversing the process we obtain a formulation for the inference. Concretely, starting from $\mathbf{z}_T \sim \mathcal{N}(\mathbf{0}, \mathbf{I})$ we can step by step recover the sample from the original distribution. We train our network to recover the original sample \mathbf{z}_0 directly as in [68] (instead of traditional formulation, in which the added noise ϵ is recovered). To achieve this, we parametrize the reverse process by a denoising neural network \mathcal{D}_{ψ} that is trained to recover the original sample \mathbf{z}_0 from the noised sample \mathbf{z}_t at timestep t given the condition c . Defining for brevity $\mathbb{E}_p \equiv \mathbb{E}_{\mathbf{z}_0 \sim p_{data}}$, $\mathbb{E}_t \equiv \mathbb{E}_{t \sim \mathcal{U}\{0, \dots, T\}}$, and $\mathbb{E}_q \equiv \mathbb{E}_{\mathbf{z}_t \sim q(\mathbf{z}_t|\mathbf{z}_0)}$ we obtain the training objective:

$$\min_{\psi} \mathbb{E}_p \mathbb{E}_t \mathbb{E}_q \|\mathcal{D}_{\psi}(\mathbf{z}_t; c, t) - \mathbf{z}_0\|. \quad (10)$$

An iterative denoising process with denoising network \mathcal{D}_ψ is defined by the following:

$$\mathbf{z}_{t-1} = \sqrt{\bar{\alpha}_{t-1}} \mathcal{D}_\psi(\mathbf{z}_t; c, t) + \sqrt{1 - \bar{\alpha}_{t-1}} \epsilon, \quad (11)$$

where $\hat{\mathbf{z}}_0 = \mathcal{D}_\psi(\mathbf{z}_t; c, t)$.

Notation. Tab. S1 defines symbols used in our work.

8. Additional evaluation

Evaluating the model with contacts conditioning. Following the evaluation of ECHO with sparse \mathcal{H} or \mathcal{O} tracking, we test the model’s performance with \mathcal{I} data provided as an additional conditioning. We report the results in Table S2. Providing contact information allows for the greatest performance improvement, compared to other modalities. This highlights that contact information plays an essential role in modeling human-object interactions.

Ablation on OMOMO. We include ablation study results on OMOMO in Table S3. We observe similar trends to the ablation results on BEHAVE.

9. Losses and Metrics

Losses. The objective function used to train our network is the weighted combination of the following losses:

$$\begin{aligned} L_n^{\mathcal{H}} &= \|\boldsymbol{\theta}_{\mathcal{H}} - \hat{\boldsymbol{\theta}}_{\mathcal{H}}\|_2 + \|\mathbf{T}_{\mathcal{H}} - \hat{\mathbf{T}}_{\mathcal{H}}\|_2 \\ L_n^{\mathcal{O}} &= \|\mathbf{T}_{\mathcal{O}} - \hat{\mathbf{T}}_{\mathcal{O}}\|_2 \\ L_n^{\mathcal{I}} &= \|\mathbf{c}_{\mathcal{I}} - \hat{\mathbf{c}}_{\mathcal{I}}\|_2 \\ L_v^{\mathcal{O}} &= \|\mathbf{V}_{\mathcal{O}} - \hat{\mathbf{V}}_{\mathcal{O}}\|_2 \\ L_j^{\mathcal{H}} &= \|\mathbf{J}_{\mathcal{H}} - \hat{\mathbf{J}}_{\mathcal{H}}\|_2 \\ L_s^{\mathcal{H}} &= \|\mathbf{c}_{\mathcal{I}}^{feet} * \hat{\mathbf{U}}_{\mathcal{H}}^{feet}\|_2 \end{aligned} \quad (12)$$

where $\hat{\mathbf{U}}_{\mathcal{H}}^{feet}$ is the velocity of predicted feet joints, and $\mathbf{c}_{\mathcal{I}}^{feet}$ is the ground-truth binary contact labels for feet. The resulting loss function is:

$$L_{ECHO} = \lambda_n^{\mathcal{H}} L_n^{\mathcal{H}} + \lambda_n^{\mathcal{O}} L_n^{\mathcal{O}} + \lambda_n^{\mathcal{I}} L_n^{\mathcal{I}} + \lambda_v^{\mathcal{O}} L_v^{\mathcal{O}} + \lambda_j^{\mathcal{H}} L_j^{\mathcal{H}} + \lambda_s^{\mathcal{H}} L_s^{\mathcal{H}} \quad (13)$$

with weighting coefficients set to: $\lambda_n^{\mathcal{H}} = \lambda_n^{\mathcal{O}} = \lambda_n^{\mathcal{I}} = 1$, $\lambda_v^{\mathcal{O}} = \lambda_j^{\mathcal{H}} = 0.1$, $\lambda_s^{\mathcal{H}} = 0.05$.

Evaluating human prediction. MPJPE measures average L2 distance between predicted $\hat{\mathbf{J}}_{\mathcal{H}}$ and ground-truth body joints $\mathbf{J}_{\mathcal{H}}$:

$$MPJPE(\mathbf{J}_{\mathcal{H}}, \hat{\mathbf{J}}_{\mathcal{H}}) = \frac{1}{|\mathbf{J}_{\mathcal{H}}|} \sum_{i \in |\mathbf{J}_{\mathcal{H}}|} \|\mathbf{J}_{\mathcal{H}}^i - \hat{\mathbf{J}}_{\mathcal{H}}^i\|_2 \quad (14)$$

MPJVE measures average velocity error for predicted $\hat{\mathbf{J}}_{\mathcal{H}}$ and ground-truth body joints $\mathbf{J}_{\mathcal{H}}$. Velocity at step i is computed as: $\mathbf{U}_{\mathcal{H}}^i = \mathbf{J}_{\mathcal{H}}^i - \mathbf{J}_{\mathcal{H}}^{i-1}$, thus we define:

$$MPJVE(\mathbf{J}_{\mathcal{H}}, \hat{\mathbf{J}}_{\mathcal{H}}) = \frac{1}{|\mathbf{J}_{\mathcal{H}}| - 1} \sum_{i \in \{1..|\mathbf{J}_{\mathcal{H}}|\}} \|\mathbf{U}_{\mathcal{H}}^i - \hat{\mathbf{U}}_{\mathcal{H}}^i\|_2 \quad (15)$$

Foot contact (FC) measures the fraction of frames with any of 4 feet joints (ankle and foot for both legs) located closer to ground than a pre-defined threshold (10 and 5 cm. respectively).

Evaluating object prediction. The E_{v2v} measures the average L2 distance between the position of the predicted object vertices and the ground truth ones:

$$E_{v2v}(\mathbf{V}_{\mathcal{O}}, \hat{\mathbf{V}}_{\mathcal{O}}) = \frac{1}{|\mathbf{V}_{\mathcal{O}}|} \sum_{i \in \{0..|\mathbf{V}_{\mathcal{O}}|\}} \|\mathbf{V}_{\mathcal{O}}^i - \hat{\mathbf{V}}_{\mathcal{O}}^i\|_2 \quad (16)$$

The E_c measures the average L2 distance between the position of the predicted object center and the ground truth one:

$$E_c(\mathbf{V}_{\mathcal{O}}, \hat{\mathbf{V}}_{\mathcal{O}}) = \left\| \frac{1}{|\mathbf{V}_{\mathcal{O}}|} \sum_{i \in \{0..|\mathbf{V}_{\mathcal{O}}|\}} \mathbf{V}_{\mathcal{O}}^i - \frac{1}{|\hat{\mathbf{V}}_{\mathcal{O}}|} \sum_{i \in \{0..|\hat{\mathbf{V}}_{\mathcal{O}}|\}} \hat{\mathbf{V}}_{\mathcal{O}}^i \right\|_2 \quad (17)$$

Rotation Difference (Rot. Diff.) measures the average angle difference between predicted global rotation for the object and the ground truth one.

Quaternion difference (Q. Diff.) measures the average L1 distance between the predicted and ground-truth quaternions for the global transformation of the object.